

1 **A web-accessible computer program for calculating electrical**
2 **potentials and ion activities at cell-membrane surfaces**

3 Peter M. Kopittke^{1,2*}, Peng Wang¹, Neal W. Menzies^{1,2}, Ravi Naidu^{2,3}, Thomas B. Kinraide⁴

4 *¹The University of Queensland, School of Agriculture and Food Sciences, St. Lucia, Queensland,*
5 *4072, Australia.*

6 *²Cooperative Research Centre for Contamination Assessment and Remediation of the Environment*
7 *(CRC-CARE), P.O. Box 486, Salisbury South, South Australia, 5106, Australia.*

8 *³University of South Australia, Centre for Environmental Risk Assessment and Remediation, Mawson*
9 *Lakes, South Australia, 5095, Australia.*

10 *⁴Agricultural Research Service, U.S. Department of Agriculture, (retired; email: tom@kinraide.net)*

11

12 *To whom correspondence should be addressed. Phone: +61 7 3346 9149, Fax: +61 7 3365
13 1177, Email: p.kopittke@uq.edu.au

14

15 **Tables: 1**

16 **Figures: 6**

17

18

19

20 **Abstract**

21 *Aims.* Increasing evidence indicates that plant responses to ions (uptake/transport, inhibition,
22 and alleviation of inhibition) are dependent upon ion activities at the outer surface of root-cell
23 plasma membranes (PMs) rather than activities in the bulk-phase rooting medium.

24 *Methods.* A web-accessible computer program was written to calculate the electrical potential
25 (ψ) at the outer surface of root-cell PMs (ψ_{PM}). From these values of ψ_{PM} , activities of ion I
26 with charge Z ($\{I^Z\}$) can be calculated for the outer surface of the PM ($\{I^Z\}_{PM}$). In addition, ψ
27 and $\{I^Z\}$ in the Donnan phase of the cell walls (ψ_{CW} and $\{I^Z\}_{CW}$) can be calculated.

28 *Results.* By reanalysing published data, we illustrate how this computer program can assist in
29 the investigation of plant-ion interactions. For example, we demonstrate that in saline
30 solutions, both Ca deficiency and Na uptake are more closely related to $\{Ca^{2+}\}_{PM}$ and
31 $\{Na^+\}_{PM}$ than to $\{Ca^{2+}\}_b$ and $\{Na^+\}_b$ (activities in the bulk-phase media). Additional examples
32 are given for Zn and P nutrition, Ni toxicity, and arsenate uptake.

33 *Conclusions.* The computer program presented here should assist others to develop an
34 electrostatic view of plant-ion interactions and to re-evaluate some commonly-held views
35 regarding mechanisms of ion transport, toxicity, competition among ions, and other
36 phenomena.

37

38 *Keywords:* electrical potential, mineral nutrition, plant growth, plant-ion interactions, plasma
39 membrane, toxicity.

40

41

42 **Introduction**

43 When considering interactions between plants and ions, plant performance has been related
44 predominantly to the concentration or activity of the ions in the bulk-phase rooting medium.
45 However, these relationships are often weak or inconsistent. For example, cations in the
46 rooting medium, especially Ca^{2+} , Mg^{2+} , and H^+ , may promote or inhibit root elongation and
47 may alleviate or enhance the phytotoxicities of ionic species of trace metals and metalloids
48 such as Al (Brady et al. 1993; Kinraide 2003b), Cu (Luo et al. 2008), Zn (Pedler et al. 2004),
49 Se (Kinraide 2003a), and As (Wang et al. 2008). In general, the interpretation of ion effects is
50 clarified by a consideration of ion activities at root-cell plasma membrane (PM) surfaces in
51 addition to ion activities in the rooting media.

52

53 The PM surface carries negative charges, thus creating a negative PM surface electrical
54 potential (ψ_{PM}) (Kinraide and Wang 2010). This negative ψ_{PM} influences the distribution of
55 ions at the PM surface by attracting cations and repelling anions. Hereafter, the activity of an
56 ion I with charge Z in the bulk-phase rooting medium will be denoted $\{I^Z\}_{\text{b}}$ whilst its activity
57 at the outer surface of the PM will be denoted $\{I^Z\}_{\text{PM}}$. $\{I^Z\}_{\text{PM}}$ is computed from ψ_{PM} and $\{I^Z\}_{\text{b}}$
58 as described later. The magnitude of ψ_{PM} is not static, rather, it is influenced by the
59 composition of the rooting medium. Increases in the concentration of cations reduce the
60 negativity of ψ_{PM} due to binding of the cations or by electrical screening (Wang et al. 2011);
61 anions have relatively small effects upon ψ_{PM} because of their usually low concentration at
62 negative PM surfaces and because of weak binding.

63

64 Whilst all cations reduce the negativity of ψ_{PM} , the magnitude of the reduction is a function of
65 ion charge and the strength of binding to the PM surface. For ions commonly encountered in

66 biological systems, the ability to reduce the negativity of ψ_{PM} follows this order: $Al^{3+} > H^+ >$
67 $Cu^{2+} > Ca^{2+} \approx Mg^{2+} > Na^+ \approx K^+$ (Kinraide 2006). ψ_{PM} is different from the transmembrane
68 potential difference (E_m) from the bulk phase of the rooting medium to the bulk phase of the
69 cell interior as commonly measured by microelectrodes (see Nobel (2009), see also Fig. 1 of
70 Kinraide (2001) or Fig. 1 of Wang et al. (2011)).

71

72 Increasing evidence indicates that plant responses to ions (uptake/transport, inhibition, and
73 alleviation of inhibition) are dependent upon $\{I^Z\}_{PM}$ rather than $\{I^Z\}_b$ (for examples, see
74 Kinraide (2006), Kopittke et al. (2011a), Kopittke et al. (2011c), Wang et al. (2008), or Wang
75 et al. (2011)). Indeed, it has been known for almost 100 years that root tissues are negatively
76 charged (Devaux 1916), and it was proposed at least 40 years ago that this negative charge
77 could possibly explain observed plant-ion interactions (for example, see van Hai and
78 Laudelout (1971)). However, the absence of a readily available, fully parameterized
79 electrostatic model for the computation of ψ_{PM} (and, consequently, $\{I^Z\}_{PM}$) has hindered
80 efforts to examine these interactions. The recent development of such models (Kinraide and
81 Wang 2010; Yermiyahu et al. 1997b) provides an opportunity to investigate the role of ψ_{PM} in
82 plant-ion interactions.

83

84 The above introduction omits any discussion of cell wall (CW) influences upon the electrical
85 properties of the PM. However, the PMs of root cells are not exposed directly (or exclusively)
86 to the rooting medium, rather, they are exposed, in part, to the Donnan phase of the CW,
87 which is in turn exposed to the rooting medium. Hence, the composition of the rooting
88 medium influences both ψ_{PM} and the potential of the CW Donnan phase (ψ_{CW}) (see Kinraide
89 (2004) for a comprehensive discussion). However, the presence of the CW has relatively

90 small effect on $\{I^Z\}_{PM}$, and ion concentrations at the PM surface modelled with and without
91 the CW are highly correlated (Kinraide 2004). Thus, for simplicity, ion activities at the PM
92 surface can be computed as though the CW were absent, which is indeed the case for the cells
93 of many organisms.

94

95 The aim of the present study is to present a WEB-accessible computer program that uses a
96 fully parameterized electrostatic model to calculate ψ for plant root cell PMs and CWs based
97 upon the composition of the rooting medium. From this, values for $\{I^Z\}_{PM}$ and $\{I^Z\}_{CW}$ can be
98 determined. In particular, we hope to increase the ease with which these calculations can be
99 conducted in order to promote their use amongst fellow scientists as well as industrial and
100 governmental technologists and regulators. In addition to electrostatic models, the computer
101 program incorporates speciation capabilities so that preliminary speciation by dedicated
102 speciation programs is not required for many applications.

103

104 Using this computer program, we present examples of how plant-ion interactions can be
105 interpreted using electrostatic theory. We have chosen to focus on plants in the present study,
106 but the computer program developed here can be applied to PMs of other organisms (Kinraide
107 2006; Wang et al. 2013).

108

109 **Materials and methods**

110 A computer program (SGCS, Speciation Gouy Chapman Stern) was written to enable users to
111 perform readily electrostatic calculations for plants growing in commonly encountered
112 solutions. The values for ψ_{PM} , $\{I^Z\}_{PM}$, and other quantities may then be used examine plant-
113 ion interactions. The program is available from the authors or from

114 www.uq.edu.au/agriculture/sgcs/. Although the program has been substantially verified in
115 terms of agreement between computed and measured values (Kinraide 2004; Kinraide and
116 Wang 2010), we intend to revise and upgrade the program as needed. We invite users to make
117 recommendations.

118

119 Microsoft Visual Basic, within Microsoft Visual Studio 2010, was used for programming.

120 The SGCS program runs on both 32-bit and 64-bit operating systems with Microsoft

121 Windows XP or later software. The code is written in three major sections; the first section

122 performs the solution speciation, the second performs the electrostatic calculations, and the

123 third provides the linkages between the graphical user interface (GUI) and the mathematical

124 calculations for speciation and electrostatics.

125

126 *Speciation*

127 This SGCS computer program does not provide comprehensive speciation capabilities (as do

128 GEOCHEM or PhreeqcI), but rather it provides speciation for the most commonly

129 encountered ions and some of their complexes. Cations in the speciation calculations include

130 Al^{3+} , Ca^{2+} , Cd^{2+} , Cu^{2+} , H^+ , K^+ , Mg^{2+} , Mn^{2+} , Na^+ , Ni^{2+} , and Zn^{2+} , while the anions include

131 AsO_4^{3-} , Cl^- , CO_3^{2-} , NO_3^- , OH^- , PO_4^{3-} , and SO_4^{2-} . A full list of included species/complexes

132 can be found within the computer program, but the list includes the complexes Al-OH, Al-

133 SO_4 , Al- PO_4 , Ca- CO_3 , Ca- SO_4 , Cd-Cl, Cd- CO_3 , Cd- SO_4 , Cu- CO_3 , Cu-OH, Cu- SO_4 , Mg- CO_3 ,

134 Mg- PO_4 , Mg- SO_4 , Mn- CO_3 , Mn- SO_4 , Ni- CO_3 , Ni- SO_4 , Zn- CO_3 , and Zn- SO_4 . Activity

135 coefficients are calculated using the extended Debye-Hückle equation (equation 2.11 of

136 Lindsay (1979)) with simplified values for the effective size ($10^8 d_i$) of hydrated ions: $d_i = 3$

137 for monovalent ions, $d_i = 6$ for divalent ions, and $d_i = 9$ for trivalent ions. When necessary, all
138 speciation constants are easily accessed and modified by the user from within the GUI.

139

140 *Electrostatic theory at the PM surface*

141 The electrostatic theory used in the development of the computer program can be expressed in
142 a few equations. Here we provide a brief synopsis of the theory as presented in detail by
143 Yermiyahu and Kinraide (2005) and Kinraide and Wang (2010). The PM is modelled as
144 though it were composed of negatively charged (R^-) and neutral (P^0) sites to which ions (I^Z)
145 may bind to form species RI^{Z-1} and PI^Z . R_T is the sum of all R sites whether free or binding an
146 ion ($R_T = R^- + RI^{Z-1}$), and P_T is the sum of all P sites whether free or binding an ion ($P_T = P^0$
147 $+ PI^Z$). Equations 1 and 2 express the binding reactions.

148



151

152 Binding constants may be expressed as

153

$$154 \quad K_{R,I} = [RI^{Z-1}] / ([R^-][I^Z]_{PM}) \quad \text{Eq. 3}$$

$$155 \quad K_{P,I} = [PI^Z] / ([P^0][I^Z]_{PM}) \quad \text{Eq. 4}$$

156

157 $[R^-]$, $[P^0]$, $[RI^{Z-1}]$, and $[PI^Z]$ denote membrane surface densities expressed in units mol m^{-2} .

158 $[I^Z]_{PM}$ denotes the concentration of the free ion at the PM surface expressed in M units. Its

159 value is computed from ion concentration in the rooting medium ($[I^Z]_b$) by a Boltzman

160 equation.

161

162
$$[I^Z]_{PM} = [I^Z]_b \exp[-Z_i F \psi_{PM}/(RT)]$$
 Eq. 5

163

164 F , R , and T are the Faraday constant, the gas constant, and the temperature, respectively; RT/F
165 = 25.7 mV at 25°C, so $-Z_i F \psi_{PM}/(RT) = -Z_i \psi_{PM}/25.7$ at 25°C for ψ_{PM} expressed in mV.

166

167 Equation 5 cannot be solved without a value for ψ_{PM} which appears also in the Gouy-
168 Chapman equation for surface charge density (σ , in units Coluombs per m² (C m⁻²)).

169

170
$$\sigma^2 = 2 \varepsilon_r \varepsilon_0 RT \Sigma_i [I^Z]_b (\exp[-Z_i F \psi_{PM}/(RT)] - 1)$$
 Eq. 6

171

172 $2 \varepsilon_r \varepsilon_0 RT = 0.00345$ at 25°C for concentrations expressed in M (ε_r is the dielectric constant for
173 water and ε_0 is the permittivity of a vacuum). σ is also equal to the sums of all PM surface
174 species (in units mol m⁻²) times the charge of each species times F (in units C mol⁻¹).

175

176
$$\sigma = \{-[R^-] + \Sigma_i (Z_i - 1)[RI^{Z-1}] + \Sigma_i Z_i [PI^Z]\} F$$
 Eq. 7

177

178 Values for ψ_{PM} are computed by incremental and progressive assignment of trial values to it
179 in Equations 5 and 6 until values for σ in Equations 6 and 7 converge. σ is the contingent
180 surface charge density and is dependent upon the bathing medium and the ion binding
181 expressed in Equations 1 and 2. The intrinsic surface charge density (σ_0) is the total charge
182 density in the absence of binding ($\sigma_0 = FR_T$). To compute the variables in Equation 7, the
183 constants σ_0 , $K_{R,I}$, $K_{P,I}$, R_T , and P_T must be known. Values for them for plants have been
184 estimated in previous studies (summarized in Kinraide and Wang (2010)). Finally, values for

185 $\{I^Z\}_{PM}$ is computed from ion activity in the rooting medium ($\{I^Z\}_b$) by the Nernst variation of
186 the Boltzman equation (Equation 5).

187

$$188 \quad \{I^Z\}_{PM} = \{I^Z\}_b \exp[-Z_i F \psi_{PM} / (RT)] \quad \text{Eq. 8}$$

189

190 *Electrostatic theory in the Donnan phase*

191 For plants, the program also permits calculation of ψ in the Donnan space (also known as free
192 space) of the CWs (ψ_{CW}). The CW was modelled initially as a Donnan phase composed of

193 immobile negatively charged (R_{CW}^-) and neutral (P_{CW}^0) sites to which ions can bind.

194 However, the experimental data indicate that H^+ binds to R_{CW}^- strongly and that all other

195 binding is relatively very weak and makes no significant contribution to ψ_{CW} (Kinraide 2004;

196 Shomer et al. 2003). Computed values for ψ_{CW} correspond well to values obtained by

197 implantations of microelectrodes into CWs and ζ -potential measurements of CW fragments

198 (Shomer et al. 2003). Ion activities in the Donnan space of CWs are calculated with a Nernst

199 equation, $\{I^Z\}_{CW} = \{I^Z\}_b \exp[-Z_i F \psi_{CW} / (RT)]$ (Nobel 2009).

200

201 **Results**

202 *Use of the computer program*

203 The graphical user interface (GUI) allows for the input and output of data as well as

204 customization of some of the model parameters. All speciation constants and binding

205 constants (for ion binding to PM sites) are easily modified from within the GUI. Similarly,

206 values for R_T and P_T ($\mu\text{mol m}^{-2}$) can be modified within the GUI.

207

208 Data can be inputted into the SGCS program by two general methods, ‘manual input’ or
209 ‘batch input’. For manual input, data for each solution must be manually entered into the
210 program and run individually, with the results displayed within the program window. For
211 batch input, data for multiple solutions can be entered into a CSV (comma-separated values)
212 file which is then imported into the program. Then, calculated values (e.g., bulk
213 concentrations, bulk activities, and PM surface activities for free ions and the most common
214 species) are written to an output CSV file designated by the user. The CSV file must have a
215 defined structure and layout (as expected by the program) and templates are provided.

216

217 For either of these input methods (manual or batch), the program can be run in two modes –
218 ‘speciation’ or ‘manual speciation’. For ‘speciation’, the program runs both the speciation and
219 electrostatic components. Hence, in ‘speciation’ mode, the total elemental concentrations are
220 inputted and speciation calculations are performed prior to the electrostatic calculations being
221 conducted. For ‘manual speciation’, the speciation component of the program is by-passed,
222 and the user must enter the concentrations of each individual ionic species manually (as
223 determined in another chemical speciation program such as PhreeqcI or GEOCHEM). These
224 values are then used directly for electrostatic calculations.

225

226 The SGCS program conducts speciation calculations for only certain elements (see above).
227 However, in order to increase the versatility of the program, it is possible to input
228 concentration values for additional ions without speciation calculations for those ions being
229 performed by the SGCS program, but these added ions are still used in the electrostatic
230 calculations. In particular, concentrations can be inputted for Ag^+ , Ba^{2+} , Co^{2+} , Cs^+ , Fe^{2+} , Fe^{3+} ,
231 Ga^{3+} , Gd^{3+} , Hg^{2+} , In^{3+} , La^{3+} , Pb^{2+} , Sc^{3+} , Sr^{2+} , and Tl^+ . For example, if the user wishes to add

232 10 μM Ag_2SO_4 to 1 mM CaCl_2 at pH 5.0, the concentration of free bulk-phase Ag^+ inputted
233 should be 9.8 μM (due to the formation of 0.2 μM AgSO_4^-) as determined by independent
234 speciation. These free ion concentrations (e.g., 9.8 μM Ag^+) are then used in electrostatic
235 calculations with their appropriate binding constants available in Kinraide (2009).

236

237 If desired, the user can balance cation/anion charge in the solutions using Cl^- . In these
238 instances Cl^- will be added to, or removed from, the solution to ensure the solution remains
239 balanced (although charge cannot be balanced if the total Cl^- required is < 0). If the user does
240 not want the charge to be balanced using Cl^- , the program will not run if the ‘charge error’ is
241 $> 30\%$, where error = $100(\text{positive} - \text{negative})/(\text{positive} + \text{negative})$. The user is also able to
242 equilibrate the solutions with atmospheric CO_2 (H_2CO_3) partial pressure if desired.

243

244 *Accuracy of the computer program*

245 Firstly, we checked the accuracy of the speciation calculations by comparing to those using
246 PhreeqI 2.17 and the MINTEQ database. The relevant constants of the MINTEQ database
247 were modified to be the same as those in the SGCS database. Three solutions were used to
248 compare the two programs, with input concentrations in μM units: Solution 1 = 5 $\text{Al}_2(\text{SO}_4)_3$,
249 1000 CaSO_4 , 10 CuSO_4 , and sufficient H_2SO_4 to reduce the pH to 4.5; Solution 2 = 375
250 CaCl_2 , 125 $\text{Ca}(\text{H}_2\text{PO}_4)_2$, 500 CaSO_4 , 5 CdCl_2 , 10 ZnCl_2 , and sufficient HCl to reduce pH to
251 5.5; Solution 3 = 660 CaCl_2 , 90 CaCO_3 , 250 CaSO_4 , 5 CdCl_2 , and 10 ZnCl_2 . Values calculated
252 using the SGCS program corresponded well to PhreeqI values, although slight differences
253 were observed with some CO_3 -species (such as CaHCO_3^+ , Table 1).

254

255 Secondly, and importantly, values for ψ_{PM} calculated using the electrostatic model outlined
256 here (Eq. 1 to Eq. 8) have been shown to correspond well to surface electrical potentials
257 measured by electrophoresis (to obtain zeta (ζ) potentials) or the surface attraction of ionic
258 dyes (Kinraide and Wang 2010; Wang et al. 2013; Wang et al. 2008).

259

260 **Discussion**

261 The SGCS computer program allows the calculation of ion activities at the outer surface of
262 the PM. ψ_{PM} is typically negative relative to the bulk medium. It therefore increases the PM-
263 surface activity of cations and reduces the PM-surface activity of anions. The extent to which
264 ions are attracted to or repelled from the PM surface depends also upon the charge of the ion
265 (see the Equations 5 and 8). For example, when $\psi_{PM} = -59.2$ mV, monovalent cations will be
266 concentrated 10-fold relative to the bulk solution, divalent cations will be concentrated 100-
267 fold, and trivalent cations will be concentrated 1,000-fold. In contrast, anions will be depleted
268 10-, 100-, or 1,000-fold. Depolarization (decrease in negativity) of the PM caused by the
269 addition of salts to the bulk solution (Fig. 1a) will reduce the concentration of cations at the
270 PM surface but will increase the concentration of anions (Fig. 1b). Thus, an increase in the
271 cation concentration in the bulk solution typically decreases the uptake and toxicity of other
272 cations. This ‘competition’ among cations based upon global (whole surface) electrostatic
273 interactions is different in principle from competition based upon site-specific interactions
274 among ions as described by the biotic ligand model (BLM) (Kinraide 2006). Furthermore,
275 interactions between cations and anions (e.g., enhancement by cations of anion uptake and
276 toxicity) can be understood by electrostatic principles but not by site-specific competitions.

277

278 Here, using the SGCS computer program, we present examples of how activities of ions at the
279 outer PM surface can be used to interpret plant-ion interactions. Although we have focused on
280 plant-ion interactions, this electrostatic theory can be used to examine interactions in other
281 species, including bacteria and animals (Kinraide 2006). The results below are presented in
282 two parts, the first examining the uptake of essential nutrient ions in the deficient to adequate
283 supply range, and the second examining the toxicity (and alleviation of toxicity) of essential
284 and non-essential ions.

285

286 *Mineral nutrition of essential cations and anions*

287 Whilst plants are selective and active in their uptake of nutrients (and different conditions
288 influence the selectivity of this uptake), we suggest that the uptake of nutrient ions is
289 influenced by the activity of the ion at the outer surface of the root cell PM, which may differ
290 greatly from its activity in the bulk-phase rooting medium.

291

292 Two cationic nutrients are examined here, the first being Zn. Chaudhry & Loneragan (1972a;
293 b) investigated the effect of Ca, Mg, Ba, Sr, and H on the absorption of Zn by wheat roots at
294 concentrations relevant for Zn nutrition (0.1 to 10 μM). The authors observed that at a
295 constant bulk concentration of Zn, increases in Ca, Mg, Ba, Sr, or H reduced the uptake of Zn
296 (Fig. 2a). For example, with 1 μM Zn in the bulk solution, a decrease in pH from 7 to 3, with
297 350 μM basal Ca, reduced Zn uptake from 430 to 3.5 $\text{ng g}^{-1} \text{d}^{-1}$. Given that the concentration
298 of Zn in solution was constant, these changes in Zn uptake induced by H cannot be explained
299 by changes in $\{\text{Zn}^{2+}\}_{\text{b}}$ (Fig. 2a). However, the increase in H^+ from 0.1 to 1000 μM activity
300 was computed to reduce the negativity of ψ_{PM} from -51 to $+33$ mV thereby reducing
301 $\{\text{Zn}^{2+}\}_{\text{PM}}$ from 45 to 0.06 μM . Therefore, we suggest that these changes in Zn uptake resulted

302 from changes in the negativity of ψ_{PM} which in turn influenced $\{Zn^{2+}\}_{PM}$. Indeed, across all
303 cations, when Zn uptake was related to $\{Zn^{2+}\}_{PM}$ rather than $\{Zn^{2+}\}_b$, the r^2 value improved
304 from 0.604 to 0.925 (Fig. 2).

305

306 Calcium was the second cationic nutrient examined. It is often reported that plant growth in
307 saline conditions is reduced because cationic salts (typically Na or Mg) compete with Ca for
308 uptake and induce Ca deficiency (Grattan and Grieve 1992; 1999). We contend that the
309 changes in Ca nutrition do not result from site-specific competition, but rather, from changes
310 in $\{Ca^{2+}\}_{PM}$ resulting from variations in ψ_{PM} . For example, Carter et al. (1979) examined the
311 influence of cations (Mg, Na, and K) on Ca deficiency for the growth of barley (*Hordeum*
312 *vulgare* L.) shoots and roots in nutrient solutions simulating saline soil solutions of Canada.
313 No significant relationship was found between dry mass and $\{Ca^{2+}\}_b$ ($r^2 = 0.442$, Fig. 3a). In
314 contrast, the data demonstrate that changes in the solution composition influenced ψ_{PM} and
315 that Ca availability was related to $\{Ca^{2+}\}_{PM}$ ($r^2 = 0.910$, Fig. 3b). Thus Ca deficiency in saline
316 soils does not result from direct competition between Ca and other cations, but rather, from a
317 non-specific, cation-induced reduction in $\{Ca^{2+}\}_{PM}$ to deficiency levels (see also Kopittke et
318 al. (2011a)).

319

320 The SGCS model was also used to investigate the role of ψ_{PM} for anionic nutrients. In contrast
321 to cationic nutrients, a reduction in the negativity of ψ_{PM} (caused by an increase in the
322 concentration of cations) is expected to increase the activity of the anionic nutrient at the PM
323 surface and hence increase uptake (Fig. 1). However, our analyses here were hindered by a
324 lack of suitable published data for nutrient anions (to be suitable, a study must examine
325 uptake across an adequate range of solution compositions). In one study, Franklin (1969)

326 studied uptake of P in excised roots of barley and found that the addition of various metals
327 influenced the uptake of P (ranging from 5 to 18 $\mu\text{g g}^{-1}$). In solutions with a constant P
328 concentration of 20 μM , the order of effectiveness upon uptake (least to greatest) was K ~ Li
329 ~ Na < Ba ~ Sr ~ Mg ~ Ca < Fe(II) < Fe(III) ~ Al. Noticeably, this effect on uptake was the
330 opposite to that observed for cationic nutrients (Fig. 2 and Fig. 3), *viz.* an increase in the
331 concentration of (depolarizing) cations increased P uptake but decreased Zn and Ca uptake.
332 However, the results of Franklin (1969) cannot be re-analysed precisely; solution pH was not
333 stated and hence the distribution among P-species (for example, HPO_4^{2-} and H_2PO_4^-) cannot
334 be calculated nor can ψ_{PM} be calculated (for some of the cations, solution pH likely varied
335 widely among treatments). Regardless, given that the total P concentration remained constant
336 in the bulk solution, it is unlikely that these changes in uptake can be explained by changes in
337 bulk activities of P species.

338

339 Significantly, the sequence of metals enhancing P uptake (K to Al above) corresponds to the
340 effectiveness with which these metals depolarize the PM (Kinraide 2009). P uptake increased
341 with the strength of metal binding to hard ligands such as the carboxylic acid groups of the
342 PM (Fig. 4). Thus P uptake was lowest in solutions containing cations that depolarize the PM
343 the least and highest in the solutions containing cations that depolarize the PM the most.
344 These results hold some significance for acidic soils that may be rich in Al and poor in
345 available P.

346

347 *Toxicity of essential and non-essential cations and anions*

348 We also used the SGCS model to investigate the phytotoxicity of essential and non-essential
349 ions. For cationic toxicants (such as Cu, Ni, or Cd), toxicity is commonly understood

350 according to the biotic ligand model (BLM) which postulates that the adverse effect of a
351 toxicant is determined by the degree of its binding to a site (the 'biotic ligand') whose
352 occupancy by the toxicant leads to the toxicity (Paquin et al. 2002). A further postulate of the
353 BLM is that the beneficial effects of ameliorating cations (such as Ca, Mg, or H) arise from
354 competition between the ameliorant and the toxicant at the biotic ligand (Di Toro et al. 2001;
355 Paquin et al. 2002; Slaveykova and Wilkinson 2005). In contrast, we postulate that the
356 principle ameliorative effect of cations such as Ca, Mg, or H can be explained, usually, by this
357 sequence: 1. Ameliorative cations reduce the negativity of ψ_{PM} . 2. The reduced negativity of
358 ψ_{PM} reduces the PM-surface activity of the cationic toxicant. 3. The reduced PM-surface
359 activity of the toxicant reduces its binding to the biotic ligand, if indeed such a ligand plays a
360 role. In some cases one or more of the steps in the sequence may not be significant. An
361 ameliorative cation may be effective at such low concentrations that neither the PM-surface
362 negativity nor the PM-surface activity of the toxicant are significantly reduced (see below).

363

364 We reanalysed the data of Wu & Hendershot (2010) who examined the influence of H and Ca
365 on the toxicity of Ni to roots of pea (*Pisum sativum* L.). The authors reported that the addition
366 of either H or Ca typically decreased the toxicity of the Ni (Fig. 5a). For example, in solutions
367 with 10 μM Ni and 2 mM Ca, relative root elongation improved from 51 % with 1 μM H^+ to
368 130 % with 100 μM H^+ (Fig. 5a). Indeed, across all treatments, the toxicity of Ni was only
369 poorly correlated with $\{\text{Ni}^{2+}\}_b$ ($r^2 = 0.580$, Fig. 5a). In contrast, the toxicity of Ni was more
370 closely correlated to $\{\text{Ni}^{2+}\}_{PM}$ ($r^2 = 0.761$, Fig. 5b), which decreased with the addition of
371 cations (Ca^{2+} or H^+).

372

373 A second cationic toxicant was examined; in saline systems, the excess salt may lead to
374 specific-ion toxicities (Munns 2002). We reanalysed the data of Davenport et al. (1997) who
375 examined the effect of Ca (0.06 to 3.1 mM) on the uptake of Na from saline solutions
376 containing 5 to 150 mM Na. As expected, the authors observed that the addition of Ca
377 reduced uptake of Na. For example, in solutions containing 110 mM $\{Na^+\}_b$, an increase in
378 Ca from 0.06 to 3.1 mM decreased Na uptake from 20 to 10 $\mu\text{mol g}^{-1} \text{root h}^{-1}$ (Fig. 6b).
379 Indeed, across all treatments, the relationship between Na uptake and $\{Na^+\}_b$ was
380 comparatively poor ($r^2 = 0.686$, Fig. 6a) – the authors stating that this Ca-induced reduction in
381 uptake was possibly due to the binding of Ca to the cation channels through which Na uptake
382 was occurring. While Ca blockade of Na-conducting channels may indeed be a factor in Na
383 uptake and toxicity, the Ca-induced reduction in $\{Na^+\}_{PM}$ is surely important; $r^2 = 0.925$ (Fig.
384 6b) for $\{Na^+\}_{PM}$ vs. Na uptake. Therefore, this ameliorative effect of Ca was in part non-
385 specific, with the addition of Ca decreasing the negativity of ψ_{PM} and hence decreasing uptake
386 by lowering the activity of Na at the PM surface. Other examples regarding the importance of
387 electrostatic interactions in regulating the toxicity of cations (including Cu, Pb, and Mn) are
388 given in Kinraide (2006), Kinraide & Wang (2010), and Kopittke et al. (2011b).
389
390 Finally, we examined the exacerbation of anion toxicity and the enhancement of uptake
391 caused by an increase in the concentration of cations as reported for selenate, SeO_4^{2-}
392 (Kinraide 2003a). These observations cannot be explained by the usual hypotheses such as
393 channel blockade. As found for anionic nutrients (see earlier), comparatively few data are
394 available for examining the effect of cations on the uptake of anionic toxicants. In a study
395 with wheat, Wang et al. (2011) found that the addition of Ca, Mg, or H slightly increased both
396 the toxicity and uptake of arsenate (AsO_4^-) (data not presented). This is in contrast to the

397 effects upon cationic toxicants such as Ni and Na (see above) where an increase in the
398 concentration of cations decreased toxicity and uptake. However, relating As uptake to
399 $\{H_2AsO_4^-\}_{PM}$ rather than $\{H_2AsO_4^-\}_b$ did not improve the r^2 value ($r^2 = 0.803$ versus 0.839).
400 This demonstrates that whilst ψ_{PM} -controlled PM-surface activities are important in regulating
401 plant-ion interactions across a range of conditions, other factors influenced by ψ_{PM} are
402 important also. Kinraide (2001) and Wang et al. (2011) provide evidence that the surface-to-
403 surface transmembrane potential difference ($E_{m,surf}$) is also influential as it provides the
404 ‘driving force’ for ion transport across the PM, but $E_{m,surf}$ becomes more negative as ψ_{PM}
405 becomes less negative. Indeed, inclusion of an additional term to account for $E_{m,surf}$ in the
406 regression analyses for arsenate uptake improved the r^2 value to 0.922 (data not presented).
407
408 The preceding discussion, examining several cationic and anionic nutrients and toxicants,
409 highlights the importance of electrostatic properties of the PM in determining the
410 bioavailability of ions. We suggest that the electrostatic properties of the root PM have a non-
411 specific effect on plant-ion interactions whereby an increase in the concentration of cations
412 decreases the negativity of ψ_{PM} (Fig. 1a) thereby decreasing the activity of cations at the PM
413 surface but increasing the activity of anions (Fig. 1b). We propose that many of the
414 ameliorative effects typically ascribed to ‘competition’ can be explained by electrostatic
415 effects. We do not, however, suggest that site-specific competition does not ever occur –
416 certainly there are examples where we would assert that competition does indeed directly
417 reduce toxicity of trace metals. For example, Zn toxicity was alleviated in wheat and radish
418 (*Raphanus sativus* L.) by 1 to 5 μM Mg, concentrations too low to affect $\{Zn^{2+}\}_b$ or $\{Zn^{2+}\}_{PM}$
419 (Zn^{2+} and Mg^{2+} have similar ionic radii) (Pedler et al. 2004). Similarly, 50 μM Mg has been
420 reported to alleviate Al toxicity in soybean, concentrations again too low to affect $\{Al^{3+}\}_b$ or

421 $\{\text{Al}^{3+}\}_{\text{PM}}$ (Silva et al. 2001). In a final example, 1 μM Cu (c. 5 μM $\{\text{Cu}^{2+}\}_{\text{PM}}$) at pH 5.6
422 strongly inhibits reproduction in free-living rhizobia, but each 0.1 unit reduction in the pH of
423 the culture medium causes a ten-fold increase in the reproduction (Kinraide and Sweeney
424 2003). These small reductions in pH cause the negativity of ψ_{PM} to decline by only 0.3 mV
425 and the $\{\text{Cu}^{2+}\}_{\text{PM}}$ to decline by only 0.1 μM . In such cases the ameliorative cation may act
426 principally as a direct competitor with the toxicant at a biotic ligand, and global electrical
427 effects may play no important role, but in our experience global electrical effects appear to
428 play the greater role, especially in the case of cationic enhancement of anion toxicity where
429 site-specific competition would appear to be unlikely. Finally, we have not considered here
430 how different plant species respond to variations in $\{I^Z\}_{\text{PM}}$, although certainly such
431 differences exist (for a detailed discussion, see Kinraide and Wang (2010)). For example, in
432 Fig. 3 it can be seen that Ca deficiency reduces the growth of barley by 10 % when $\{\text{Ca}^{2+}\}_{\text{PM}}$
433 < ca. 4 mM. However, other species have different thresholds: growth of cowpea roots was
434 decreased at ≤ 1.6 mM (Kopittke et al. 2011a), wheat roots at ≤ 0.76 mM (Kinraide 1999),
435 pea (*Pisum sativum* L.) roots at ≤ 6 mM (Wang et al. 2010), and melon (*Cucumis melo* L.)
436 roots at ≤ 15 mM (Yermiyahu et al. 1997a). Such variations need to be taken into account.

437

438 We hope that the WEB-accessible SGCS computer program described here will increase the
439 ease with which electrostatic calculations can be performed, thereby allowing further
440 investigation of the role of electrostatics in plant-ion interactions across a wide range of
441 situations.

442

443 **Acknowledgments**

444 Dr Kopittke is the recipient of an Australian Research Council (ARC) Future Fellowship
445 (FT120100277). Dr Wang is a recipient of an ARC Discovery Early Career Researcher
446 Award (DE130100943).

447

448 **References**

449 Brady D J, Edwards D G, Asher C J and Blamey F P C 1993 Calcium amelioration of
450 aluminium toxicity effects on root hair development in soybean (*Glycine max* (L.)
451 Merr.). *New Phytol* 123, 531-538.

452 Carter M R, Webster G R and Cairns R R 1979 Calcium deficiency in some Solonetzic soils
453 of Alberta. *J Soil Sci* 30, 161-174.

454 Chaudhry F M and Loneragan J F 1972a Zinc absorption by wheat seedlings and the nature of
455 its inhibition by alkaline earth cations. *J Exp Bot* 23, 552-560.

456 Chaudhry F M and Loneragan J F 1972b Zinc absorption by wheat seedlings. 2. Inhibition by
457 hydrogen ions and by micronutrient cations. *Soil Sci Soc Am Proc* 36, 327-331.

458 Davenport R J, Reid R J and Smith F A 1997 Sodium-calcium interactions in two wheat
459 species differing in salinity tolerance. *Physiol Plant* 99, 323-327.

460 Devaux H 1916 Action rapide des solutions salines sur les plantes vivantes: déplacement
461 réversible d'une partie des substances basiques contenues dans la plante. *Comptes*
462 *rendus hebdomadaires des séances de l'Académie des sciences* 162, 561-564.

463 Di Toro D M, Allen H E, Bergman H L, Meyer J S, Paquin P R and Santore R C 2001 Biotic
464 ligand model of the acute toxicity of metals. 1. Technical basis. *Environ Toxicol*
465 *Chem* 20, 2383-2396.

466 Franklin R E 1969 Effect of adsorbed cations on phosphorus uptake by excised roots. *Plant*
467 *Physiol* 44, 697-700.

468 Grattan S R and Grieve C M 1992 Mineral element acquisition and growth response of plants
469 grown in saline environments. *Agric Ecosyst Environ* 38, 275-300.

470 Grattan S R and Grieve C M 1999 Salinity-mineral nutrient relations in horticultural crops.
471 *Sci Hortic* 78, 127-157.

472 Kinraide T B 1999 Interactions among Ca^{2+} , Na^+ and K^+ in salinity toxicity: quantitative
473 resolution of multiple toxic and ameliorative effects. *J Exp Bot* 50, 1495-1505.

474 Kinraide T B 2001 Ion fluxes considered in terms of membrane-surface electrical potentials.
475 *Aust J Plant Physiol* 28, 607-618.

476 Kinraide T B 2003a The controlling influence of cell-surface electrical potential on the uptake
477 and toxicity of selenate (SeO_4^{2-}). *Physiol Plant* 117, 64-71.

478 Kinraide T B 2003b Toxicity factors in acidic forest soils: Attempts to evaluate separately the
479 toxic effects of excessive Al^{3+} and H^+ and insufficient Ca^{2+} and Mg^{2+} upon root
480 elongation. *Eur J Soil Sci* 54, 323-333.

481 Kinraide T B 2004 Possible influence of cell walls upon ion concentrations at plasma
482 membrane surfaces. Toward a comprehensive view of cell-surface electrical effects
483 upon ion uptake, intoxication, and amelioration. *Plant Physiol* 136, 3804-3813.

484 Kinraide T B 2006 Plasma membrane surface potential (ψ_{PM}) as a determinant of ion
485 bioavailability: A critical analysis of new and published toxicological studies and a
486 simplified method for the computation of plant ψ_{PM} . *Environ Toxicol Chem* 25, 3188-
487 3198.

488 Kinraide T B 2009 Improved scales for metal ion softness and toxicity. Environ Toxicol
489 Chem 28, 525-533.

490 Kinraide T B and Sweeney B K 2003 Proton alleviation of growth inhibition by toxic metals
491 (Al, La, Cu) in rhizobia. Soil Biol Biochem 35, 199-205.

492 Kinraide T B and Wang P 2010 The surface charge density of plant cell membranes (σ): an
493 attempt to resolve conflicting values for intrinsic σ . J Exp Bot 61, 2507-2518.

494 Kopittke P M, Blamey F P C, Kinraide T B, Wang P, Reichman S M and Menzies N W 2011a
495 Separating multiple, short-term deleterious effects of saline solutions to the growth of
496 cowpea seedlings. New Phytol 189, 1110-1121.

497 Kopittke P M, Blamey F P C, Wang P and Menzies N W 2011b Calculated activity of Mn^{2+} at
498 the outer surface of the root cell plasma membrane governs Mn nutrition of cowpea
499 seedlings. J Exp Bot 62, 3993-4001.

500 Kopittke P M, Kinraide T B, Wang P, Blamey F P C, Reichman S M and Menzies N W 2011c
501 Alleviation of Cu and Pb rhizotoxicities in cowpea (*Vigna unguiculata*) as related to
502 ion activities at root-cell plasma membrane surface. Environ Sci Technol 45, 4966–
503 4973.

504 Lindsay W L 1979 Chemical Equilibria in Soils. John Wiley & Sons, New York, NY, USA.
505 pp. 449.

506 Luo X S, Li L Z and Zhou D M 2008 Effect of cations on copper toxicity to wheat root:
507 Implications for the biotic ligand model. Chemosphere 73, 401-406.

508 Munns R 2002 Comparative physiology of salt and water stress. Plant Cell Environ 25, 239-
509 250.

510 Nobel P S 2009 *Physicochemical and Environmental Plant Physiology*. John Wiley & Sons,
511 New York, NY, USA.

512 Paquin P R, Gorsuch J W, Apte S, Batley G E, Bowles K C, Campbell P G C, Delos C G, Di
513 Toro D M, Dwyer R L, Galvez F, Gensemer R W, Goss G G, Hogstrand C, Janssen C
514 R, McGeer J C, Naddy R B, Playle R C, Santore R C, Schneider U, Stubblefield W A,
515 Wood C M and Wu K B 2002 The biotic ligand model: a historical overview. *Comp*
516 *Biochem Physiol C-Toxicol Pharmacol* 133, 3-35.

517 Pedler J F, Kinraide T B and Parker D R 2004 Zinc rhizotoxicity in wheat and radish is
518 alleviated by micromolar levels of magnesium and potassium in solution culture. *Plant*
519 *Soil* 259, 191-199.

520 Shomer I, Novacky A J, Pike S M, Yermiyahu U and Kinraide T B 2003 Electrical potentials
521 of plant cell walls in response to the ionic environment. *Plant Physiol* 133, 411-422.

522 Silva I R, Smyth T J, Israel D W, Raper C D and Rufty T W 2001 Magnesium is more
523 efficient than calcium in alleviating aluminum rhizotoxicity in soybean and its
524 ameliorative effect is not explained by the Gouy-Chapman-Stern model. *Plant Cell*
525 *Physiol* 42, 538-545.

526 Slaveykova V I and Wilkinson K J 2005 Predicting the bioavailability of metals and metal
527 complexes: Critical review of the biotic ligand model. *Environ Chem* 2, 9-24.

528 van Hai T and Laudelout H 1971 Phosphate uptake and root electrical potential. *J Exp Bot* 22,
529 830-&.

530 Wang P, Kinraide T B, Smolders E, Zhou D M, Menzies N W, Thakali S, Xia W W, Hao X
531 Z, Peijnenburg W J G M and Kopittke P M 2013 Development of an electrostatic

532 model predicting Cu and Ni toxicity to microbial processes in soils. *Soil Biology &*
533 *Biochemistry* 57, 720-730.

534 Wang P, Kinraide T B, Zhou D M, Kopittke P M and Peijnenburg W J G M 2011 Plasma
535 membrane surface potential: Dual effects upon ion uptake and toxicity. *Plant Physiol*
536 155, 808-820.

537 Wang P, Zhou D M, Kinraide T B, Luo X S, Li L Z, Li D D and Zhang H L 2008 Cell
538 membrane surface potential (ψ_0) plays a dominant role in the phytotoxicity of copper
539 and arsenate. *Plant Physiol* 148, 2134-2143.

540 Wang P, Zhou D M, Peijnenburg W J G M, Li L Z and Weng N 2010 Evaluating mechanisms
541 for plant-ion (Ca^{2+} , Cu^{2+} , Cd^{2+} or Ni^{2+}) interactions and their effectiveness on
542 rhizotoxicity. *Plant Soil* 334, 277-288.

543 Wu Y and Hendershot W H 2010 The effect of calcium and pH on nickel accumulation in and
544 rhizotoxicity to pea (*Pisum sativum* L.) root: Empirical relationships and modeling.
545 *Environ Pollut* 158, 1850-1856.

546 Yermiyahu U and Kinraide T B 2005 Binding and electrostatic attraction of trace elements to
547 plant-root surfaces. In *Biogeochemistry of Trace Elements in the Rhizosphere*. Eds. P
548 M Huang and G R Gobran. pp 365-389. Elsevier, Amsterdam.

549 Yermiyahu U, Nir S, BenHayyim G, Kafkafi U and Kinraide T B 1997a Root elongation in
550 saline solution related to calcium binding to root cell plasma membranes. *Plant Soil*
551 191, 67-76.

552 Yermiyahu U, Rytwo G, Brauer D K and Kinraide T B 1997b Binding and electrostatic
553 attraction of lanthanum (La^{3+}) and aluminum (Al^{3+}) to wheat root plasma membranes.
554 *J. Membrane Biol.* 159, 239-252.

555

556

557

Table 1. Comparison of speciation calculations performed either with the SGCS program or with PhreeqcI 2.17 using the Minteq database modified so that the selected constants equalled those in the default SGCS database. Data in the table are presented as ionic activities (μM). Three solutions were examined, with input concentrations of (μM): Solution 1 = 5 $\text{Al}_2(\text{SO}_4)_3$, 1000 CaSO_4 , 10 CuSO_4 , and sufficient H_2SO_4 to reduce the pH to 4.5; Solution 2 = 375 CaCl_2 , 125 $\text{Ca}(\text{H}_2\text{PO}_4)_2$, 500 CaSO_4 , 5 CdCl_2 , 10 ZnCl_2 , and sufficient HCl to reduce pH to pH 5.5; Solution 3 = 660 CaCl_2 , 90 CaCO_3 , 250 CaSO_4 , 5 CdCl_2 , and 10 ZnCl_2 . Only selected ionic species are shown.

	Solution 1		Solution 2		Solution 3	
	SGCS	PhreeqcI	SGCS	PhreeqcI	SGCS	PhreeqcI
Al^{3+}	2.9	2.9	0	0	0	0
AlOH^{2+}	0.9	0.9	0	0	0	0
$\text{Al}(\text{OH})_2^+$	0.2	0.2	0	0	0	0
AlSO_4^+	3.2	3.2	0	0	0	0
Ca^{2+}	700	700	740	740	770	770
CaHCO_3^+	0	0	0	0	1.8	1.4
CaHPO_4^0	0	0	1.5	1.8	0	0
$\text{CaH}_2\text{PO}_4^+$	0	0	4.2	4.2	0	0
CaSO_4^0	101	100	53	52	27	27
Cd^{2+}	0	0	3.4	3.4	3.4	3.3
CdCl^+	0	0	0.3	0.3	0.4	0.4
CdSO_4^0	0	0	0.3	0.3	0.2	0.2
Cl^-	0	0	770	780	1400	1400
Cu^{2+}	6.9	6.8	0	0	0	0
CuSO_4^0	1.1	1.1	0	0	0	0
H^+	34	34	3.4	3.4	0.033	0.033
HPO_4^{2-}	0	0	3.8	4.5	0	0
H_2PO_4^-	0	0	220	220	0	0
SO_4^{2-}	930	930	450	450	220	220
Zn^{2+}	0	0	7.4	7.4	7.2	7.0
ZnHCO_3^+	0	0	0	0	0.2	0.1
ZnCO_3^0	0	0	0	0	0.4	0.3
ZnSO_4^0	0	0	0.6	0.5	0.3	0.3

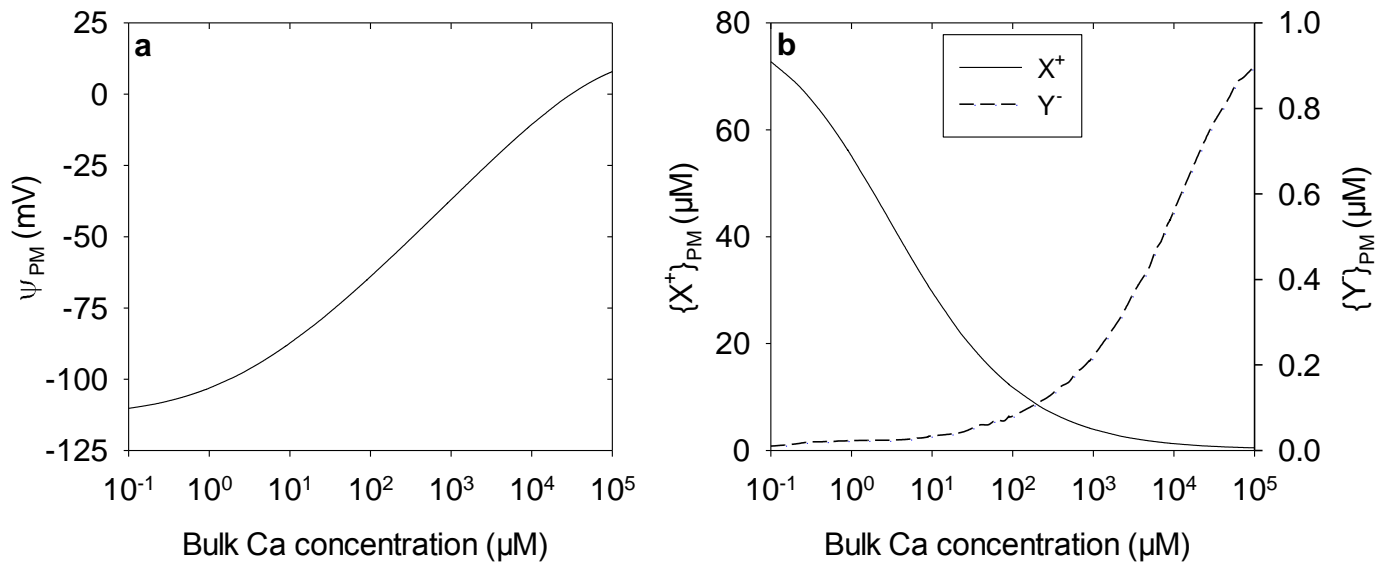


Fig. 1 (a) Electrical potential at the outer surface of the root PM (ψ_{PM}) exposed to CaCl_2 solutions at pH 5.6. (b) Activities of a monovalent cation (X^+) and a monovalent anion (Y^-) at the outer surface of the PM, when the concentrations of those ions in the bulk solution are 1 μM . Note that, compared to the bulk solution, negative values for ψ_{PM} increase the activity X^+ at the PM surface ($\{X^+\}_{PM}$) but decrease the activity of Y^- at the PM surface ($\{Y^-\}_{PM}$)

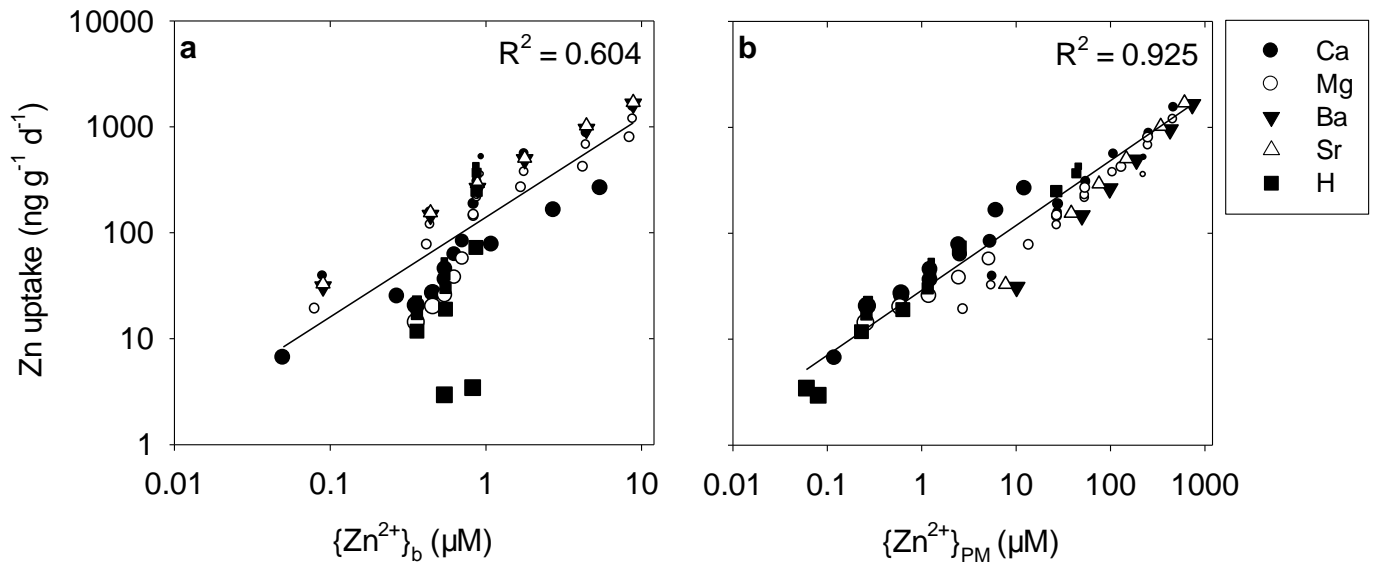


Fig. 2 Effect of Ca, Mg, Ba, Sr, and H (pH) on the absorption of Zn by wheat seedlings related to the activity of Zn²⁺ in the bulk solution (a) or at the outer surface of the root PM (b). Data were taken from Fig. 4 of Chaudhry & Loneragan (1972b) for H and from Table 1 and Fig. 2 of Chaudhry & Loneragan (1972a) for the other cations (data are excluded from the highest Ca and Mg treatments due to deleterious osmotic effects). Other than for the H⁺-treatments, a constant pH of 5.6 was assumed. The size of the symbols is proportional to the concentration of the cation

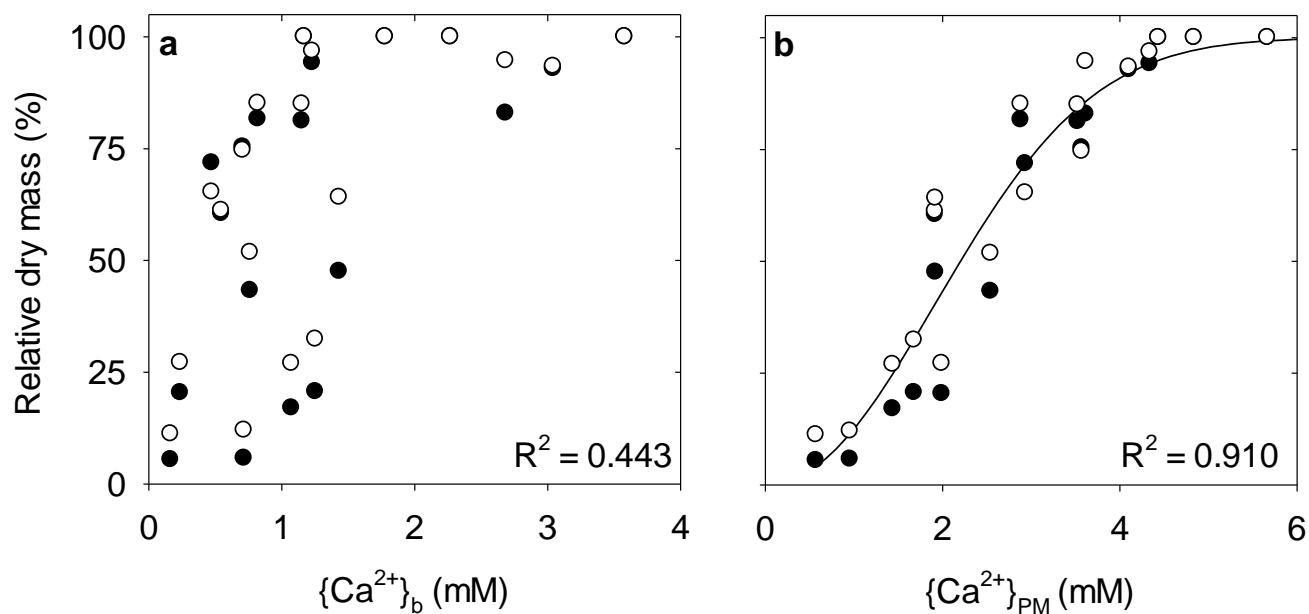


Fig. 3 The relative dry mass of shoots (●) and roots (○) of barley (*Hordeum vulgare* L.) grown in nutrient solutions for three to four weeks as related to the activity of Ca^{2+} in the bulk solution (a), or at the outer surface of the root PM (b). The solutions were at pH 5.5 and contained 0.5 to 10 mM Ca, 1.5 to 90 mM Na, 0.8 to 6.0 mM K, and 0.25 to 15.5 mM Mg. Data were taken from Experiments 1 to 4 of Carter et al. (1979)

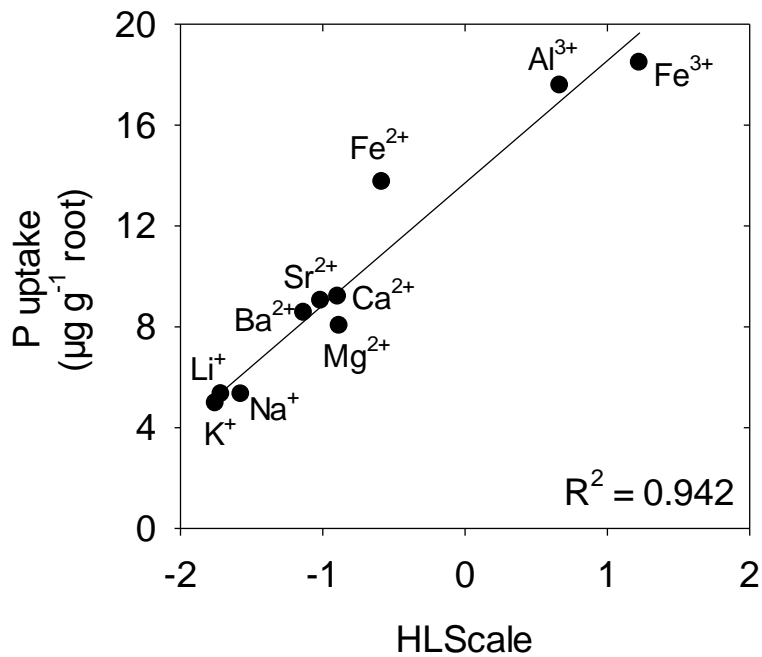


Fig. 4 The uptake of P by excised roots of barley (*Hordeum vulgare* L.) related to the Hard Ligand Scale (HLScale) for ten metals. The HLScale is a logarithmic scale of binding strength between metals and hard ligands such as the carboxylic acid groups of the PM. Thus the HLScale is a measure of the effectiveness with which cations reduce the surface negativity of the PM (Kinraide 2009). Data for P uptake are taken from Franklin (1969)

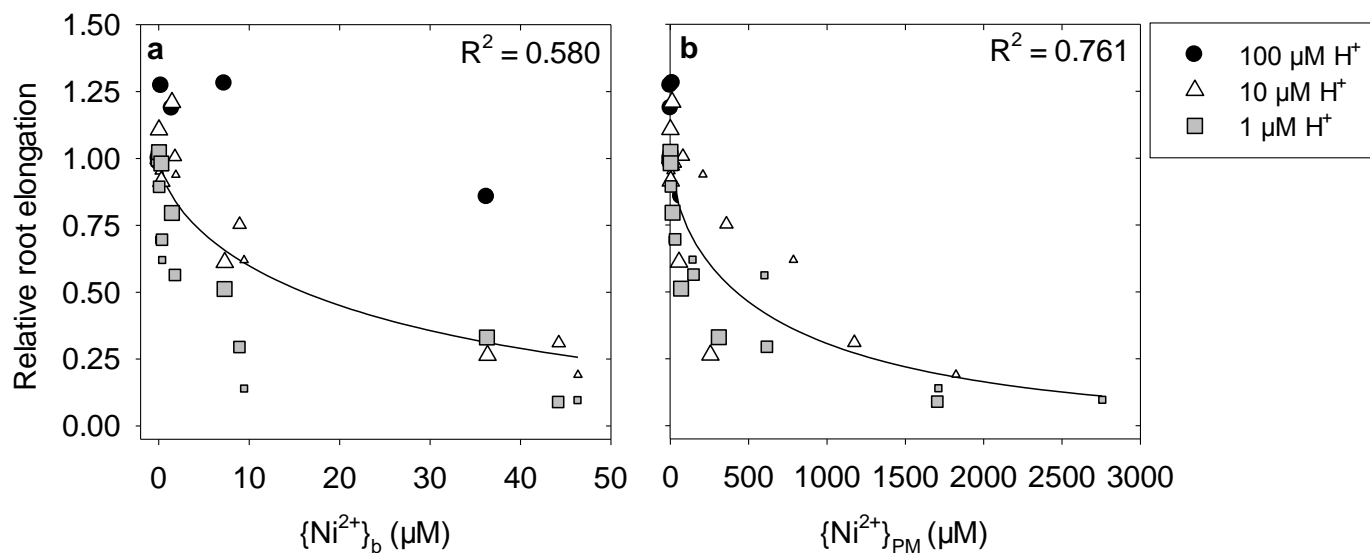


Fig. 5 Growth of pea roots in solutions with toxic levels of Ni related to the activity of Ni^{2+} in the bulk solution (a) or at the outer surface of the root PM (b). Solution pH values were 4, 5, or 6 with Ca concentration at 0.04 mM (small symbols), 0.2 mM (medium symbols), or 2 mM (large symbols). Data were taken from Table 1 of Wu and Hendershot (2010) with the pH 4 treatments at 0.04 and 0.2 mM Ca excluded due to poor root growth (> 80 % reduction when compared to other treatments)

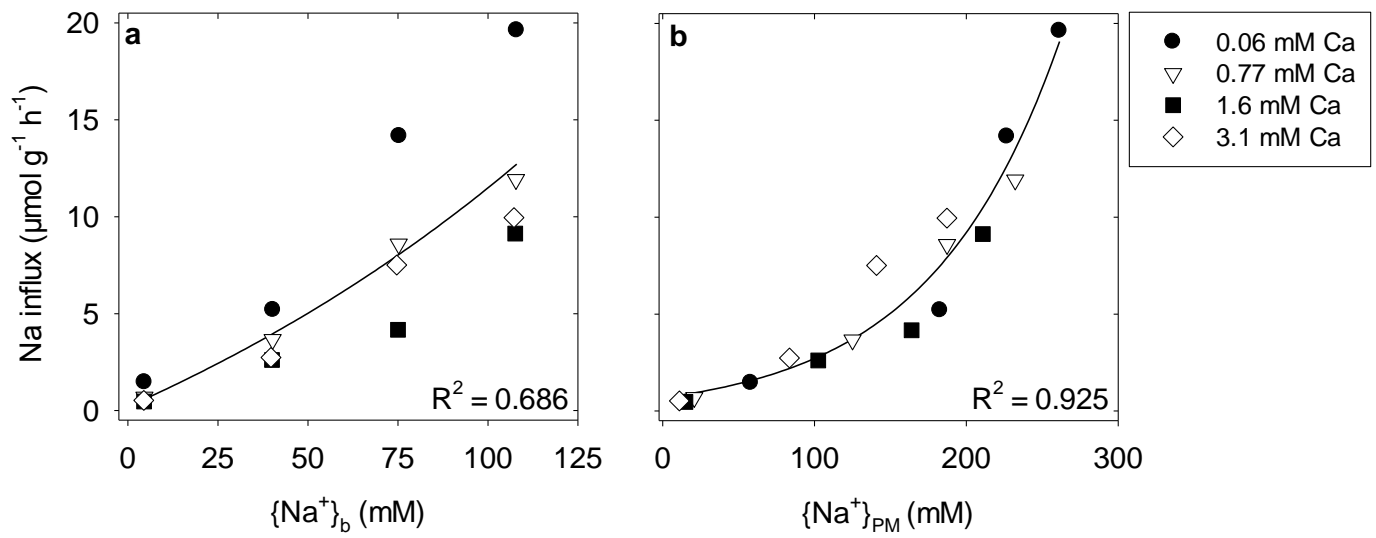


Fig. 6 Effect of Ca on the short-term influx of Na in roots of *Triticum aestivum* L. cv Kharchia, related to the activity of Na^+ in the bulk solution (a) or at the outer surface of the root PM (b). Data were taken from Fig. 2 of Davenport et al. (1997), with all solutions at pH 6.5